Received: September 12, 2023 | Revised: November 2, 2023 | Accepted: November 2, 2023

JOURNAL OF APPLIED RESEARCH ON SCIENCE AND TECHNOLOGY
JARST
INSTITUTE OF RESEARCH AND DEVELOPMENT
RAJAMANGALA UNIVERSITY OF TECHNOLOGY THANYABURI
ISSN ONLINE: 2773-9473
https://ph01.tci-thaijo.org/index.php/rmutt-journal

Cellulose rubber foam composite use as oil absorbent

Poptorn Klaykhem[1], Pruttipong Pantamanatsopa[1,2] and Warunee Ariyawiriyanan[1,3*]

[1]Department of Materials and Metallurgical Engineering, Faculty of Engineering, Rajamangala University of Technology Thanyaburi, Pathum Thani 12110, THAILAND

[2]Department of Industrial Engineering, Faculty of Engineering, Rajamangala University of Technology Srivijaya, Songkhla 90000, THAILAND

[3]Systems Research and Innovation Development Research Unit, Rajamangala University of Technology Thanyaburi, Pathum Thani 12110, THAILAND

[*]Corresponding author: warunee.a@en.rmutt.ac.th

ABSTRACT

The focus of this study was to explore the fabrication of cellulose rubber foam (CRF) using kapok fibers (KF) as an oil absorbent material. Chemical methods such as sodium hydroxide surface treatment, hydrogen peroxide treatment, and acid hydrolysis were employed to prepare cellulose nanocrystals (CNC). The results of the nuclear magnetic resonance (NMR) spectroscopy test indicated that the chemical modification of kapok fiber resulted in the removal of lignin and hemicellulose by a disappearing peak at 17, 52, and 148 ppm, respectively. Hydrolysis process of the kapok fiber resulted in nanometer-sized cellulose, with a yield of 72% as revealed by transmission electron microscopy (TEM). The amount of cellulose nanocrystals from kapok fiber (KF-CNC) used in the study varied from 0 to 5 phr during the formation of the cellulose rubber foam, and it was found that the foam density increased as the number of cellulose nanocrystals from kapok fiber increased. Additionally, the percentage of collapse from the compressive strength of cellulose rubber foam decreased as the amount of cellulose nanocrystals from kapok fiber increased. Fourier transform infrared spectroscopy (FTIR) confirmed the incorporation of cellulose nanocrystals from kapok fiber into the rubber foam (RF) as the amount of cellulose nanocrystals from kapok fiber increased. The oil absorbent of cellulose rubber foam composite with 1 phr cellulose nanocrystals from kapok fiber show highest absorption capacity was 17.8 g/g. The cellulose rubber foam composite absorbs oil before absorbing water when water and oil are combined. Moreover, the cellulose rubber foam could be reused more than 50 times.

Keywords: Kapok fiber, Rubber foam, Cellulose nanocrystals, Cellulose rubber foam, Oil absorbent

INTRODUCTION

Nowadays, the problem of natural oil contamination is still a big problem everywhere in the world and humans are involved due to the use of oil in everyday life. The leakage or contamination of oil may affect nature. The water source is the habitat of various living things, including human water resources. Many materials are used to eliminate the problem of oil contamination in water supplies. Most commercial adsorbents used in oil removal are plastic-based materials with a lot of porosity. Commercial materials may increase plastic waste that is difficult to biodegrade. Absorbent materials made from natural materials can help reduce the problem of plastic waste even more. The material that can be developed as an absorbent material is natural rubber. Thailand is the world's number one natural rubber producer but most of them are exported in the form of raw latex. Therefore, the processing of natural rubber into products may increase the benefits of using more widely available rubber. Rubber foam is a porous, lightweight material that can be used in a wide range of applications such as absorbents, cushioning materials and sound-absorbing materials, etc. [1, 2].

Composite material made from natural fibers has received widespread attention both in plastic molding industry instead of using synthetic fibers. The advantages of natural fibers are that they are cheap and easily found naturally with low toxicity. There are many natural fibers that are plentiful in Thailand such as water hyacinth, bamboo, rice husk, bagasse, etc. [3]. And there is another type that is abundant in Thailand but is still rarely used is kapok fiber. Kapok in the form of stuffed pillows, because it is light and soft, is one of the high cellulose fibers. Kapok fibers have interesting properties for example natural skin coatings. This will prevent water so that the cotton fibers do not get wet but have oil-absorbing

DOI: 10.60101/jarst.2023.254006

properties which can be applied to many aspects of work such as the environment including various oil stains occurring in daily life, etc. Therefore, it is interesting to bring local resources and develop them into oil-absorbing cellulose rubber foam. Therefore, in this research, we are interested in using natural fibers, kapok fibers which are relatively high cellulose fibers as an oil-absorbing material. In the previous work, the oil absorbency is supplemented by the addition of kapok fibers in larger quantities, resulting in a significant increase in oil absorbency [4]. However, using natural fibers may have a detrimental effect on the properties of the material. Kapok fibers must therefore be cleaned by bleaching them with hydrogen peroxide and sodium hydroxide to remove impurities or unwanted substances such as hemicellulose, lignin, and other impurities. Cellulose is hydrolyzed with acid in sulfuric acid [5] and then mixed with natural rubber foam and cellulose nanocrystals from kapok fibers with different cellulose nanocrystal contents.

MATERIALS AND METHODS

Materials

Kapok fiber (KF), HANR 60% DRC (NORRAWAT CHEMICAL Part., Ltd.), Chemicals used include sodium hydroxide (NaOH), hydrogen peroxide (H_2O_2), sulfuric acid 98% (H_2SO_4), potassium hydroxide (KOH), zinc diethyl-dithiocarbamate dispersion (ZDEC), zinc mercaptobenzo-thiazole dispersion, (ZMBT), Wingstay L, Potassium Oleate, Diphenyl guanidine (DPG), Sodium silicofluoride (SFF), Zinc oxide (ZnO)

KF pretreatment process

The KF was boiled in a 2M NaOH solution at 90 °C for 60 minutes and filtered by a sieve (involved in alkalization at mm openings) and washed with deionized (DI) water to remove NaOH. Then, the kapok alkaline fiber was subsequently bleached using 0.05 M aqueous NaOH buffer and 10% v/v aqueous H_2O_2 at 90 °C for 120 minutes with constant mechanical stirring. The bleached KF was then sieved and thoroughly washed with DI water. To further remove the impurities, the second bleaching was carried out under the same conditions and oven-dried at 60 °C for 24 hours. The bleached kapok is labeled KF-B. The alkalization and bleaching were undertaken to remove impurities before proceeding with the hydrolysis.

Isolation of KF-CNC

CNC was prepared by sulfuric acid hydrolysis [6]. The KF-B was subsequently hydrolyzed by using a diluted H_2SO_4 solution (50% v/v) at 600 rpm, 50 °C for 40 minutes. The hydrolysis was stopped by adding 200 mL of water. The resulting suspension was centrifuged five times at 9,000 rpm, 25°C for 10 minutes to obtain more concentrated cellulose nanocrystal water and centrifuged at 10°C for 50 minutes until KF-CNC deposits were obtained.

Preparation of Rubber Foam (RF) and Cellulose Rubber Foam (CRF)

The preparation of RF and CRF is shown in Table 1. The concentrated natural latex (60% DRC) was stirred for 1 minute to remove ammonia and mixing process for CRF compound preparation is shown in Table 2. Then, pour the latex into the mold and leave the RF set for 10 minutes. The prepared RF was baked at 100 °C for 2 hours, then wash with hot water at 70 °C for 50 minutes and bake again at 80 °C until dry shown in figure 1.

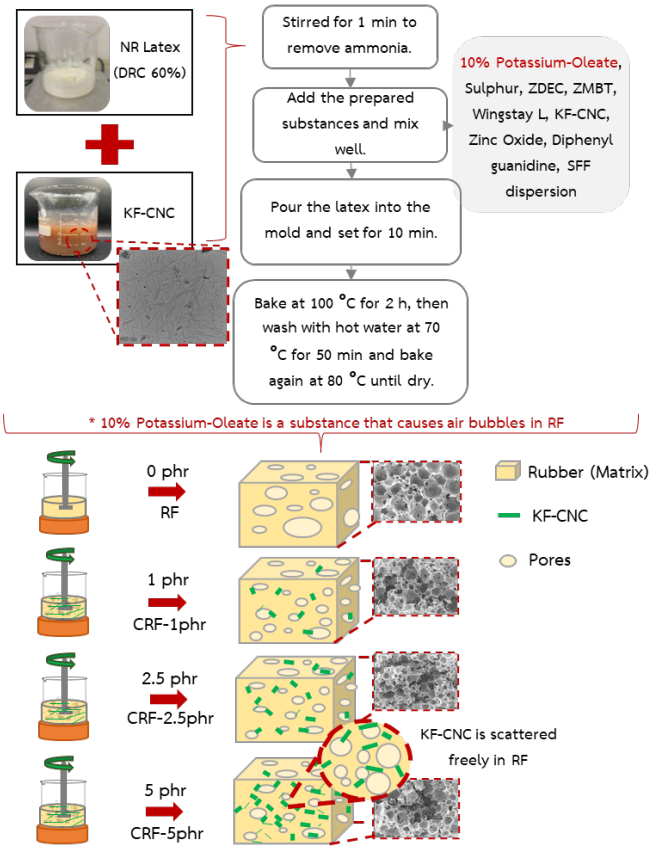

Figure 1 Images of preparation of RF and CRF.

Table 1 Formulations of RF and CRF.

Chemical substances	Weight (phr)
NR latex 60% DRC	100
Potassium-Oleate solution 10%	1.0
Sulphur dispersion 50%	2.5
ZDEC dispersion 50%	1.0
ZMBT dispersion 50%	1.0
Wingstay L dispersion 50%	1.0
ZnO dispersion 50%	5.0
Diphenyl guanidine dispersion 33%	1.0
Sodium silicofluoride dispersion 12.5%	0.5
KF-CNC	0, 1, 2.5, 5

DOI: 10.60101/jarst.2023.254006

JOURNAL OF APPLIED RESEARCH ON SCIENCE AND TECHNOLOGY

Table 2 Mixing procedure for CRF compound preparation.

Order	Ingredient	Mixing time (Minutes)
1	Latex (DRC 60%)	1
2	10% Potassium-Oleate, Sulphur, ZDEC, ZMBT, Wingstay L, KF-CNC	3
3	Zinc Oxide, Diphenyl guanidine	1
4	SFF dispersion	1

Yield of KF-CNC

The yield of KF-CNC of the dry weight ratio between KF-CNC and KF-B [7] (Equation 1), where W_{KF-CNC} was the dry weight of KF-CNC and W_{KF-B} was the dry weight of KF-B. The yield value was obtained from an average of three replications.

$$\text{Yield of KF-CNC (\%)} = \frac{W_{KF-CNC}}{W_{KF-B}} \times 10 \quad (1)$$

Chemical composition of KF-CNC, RF and CRF

The chemical composition was analyzed by Fourier transform infrared spectroscopy (FTIR; Frontier, Perkin Elmer) and nuclear magnetic resonance (NMR) spectroscopy (JEOL; JNM-ECZR 500MHz). Prior to the FTIR and NMR analyses, samples of KF-CNC, RF and CRF were oven-dried at 60 °C for 2 hours. for produce dried film. The dried samples were then scanned using the FTIR spectrometer in attenuated total reflectance mode at 4000 and 600 cm^{-1} and the NMR spectrometer in ^{13}C solid state with a chemical shift between 0-200 ppm.

Morphology of KF, KF-B, KF-CNC, RF and CRF

The morphology of KF, KF-B, RF and CRF was characterized by a scanning electron microscope (SEM) (JEOL; JSM-5410 LV). SEM was utilized to determine the dimensions and physical appearance of raw KF, KF-B, RF and CRF. Prior to SEM analysis the raw KF, KF-B, RF and CRF were stuck to the stub with carbon tape and then coated with gold. The morphology of KF-CNC was characterized by a transmission electron microscope, TEM (TEM; Thermo Scientific, TALOS F200X). TEM was utilized to determine the dimensions (i.e., diameter and length) and the physical appearance of KF-CNC. Specimen preparation prior to analysis was done by dropping KF-CNC solution on the surface of carbon grid and leaving it to dry at room temperature.

Compression testing of RF and CRF

The compression testing was conducted according to ASTM D 395 standard [8]. Prior to test cutting a circular specimen with a diameter of 29 mm, height of 19 mm, placing the specimen in a compressed steel plate, pressing to deflate 50% from its original height and holding for about 15 minutes and bake at 70 °C for 22 hours, remove from the oven. Place the specimen for 30 minutes, then measure the height of the specimen. The calculation formula is as shown in (Equation 2).

$$\text{Compression set \%} = \left(\frac{t_0 - t}{t_0}\right) \times 100 \quad (2)$$

Where t_0 = thickness after test (mm) and t = original thickness (mm)

Density of RF and CRF

The density analysis was performed according to the ASTM D 3574-95 standard [9]. Prior to test cutting a rectangular piece of CRF. Weight and calculate the density of the sample using the formula as in (Equation 3).

$$D = \frac{M}{V} \quad (3)$$

Where D= density of specimen (g/cm^3), M= specimen weight (g) and V= specimen volume (cm^3)

Ability to oil absorbent of RF and CRF

The ability to absorb oil for RF and CRF analysis is determined by cutting the test specimen to a size of 2.5x2.5x2.5 cm then dropping the sample into the beaker with the oil at varying time with 15, 30, 60, 120, 180 and 1440 minutes, respectively. Then, take the sample out of the oil beaker. Clean the oil on the surface of the CRF. Then weigh and calculate the adsorption capacity (oil sorption capacity) in (Equation 4) [10].

$$\text{Oil sorption capacity (g/g)} = \frac{Ms - Mi}{Mi} \quad (4)$$

Where M_s = weight after adsorption (weight of RF and CRF and oil in grams) and M_i = weight before adsorption (RF and CRF weight in grams).

RESULTS AND DISCUSSION

KF preparation results

Figure 2a and 2b are the photographs of KF and KF-B. In figure 2a, the color of RF is light brown. Figure 2b shows the KF-B, the color of KF-B is white. The change in color was confirmed by the removal of wax, lignin, hemicellulose and other impurities following the chemical treatment (alkalinization and bleaching).

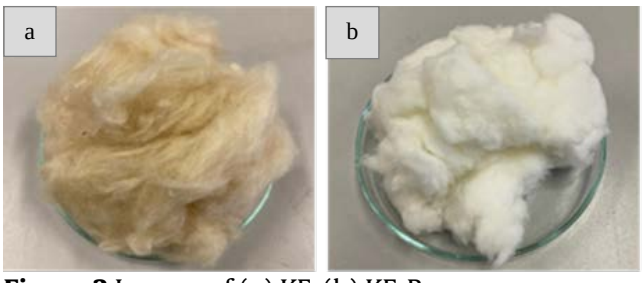

Figure 2 Images of (a) KF, (b) KF-B.

DOI: 10.60101/jarst.2023.254006

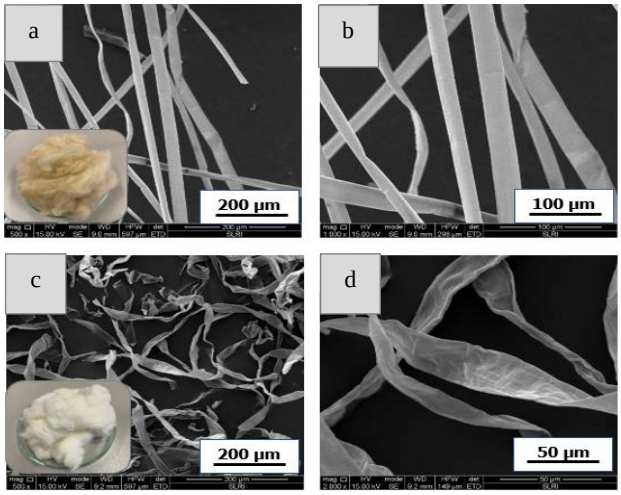

Figure 3 The morphological test results of (a,b) KF, (c,d) KF-B were observed using a scanning electron microscopy (SEM).

Morphology results of KF and KF-B

Figure 3a-3d show the microstructure of KF and KF-B by using SEM. In Figure 3a and 3b, the KF was bundled together and the fibers are thick. Following the alkalization and KF-B. In Figure 3c-3d bleaching future thinned out the fibers, resulting in the microfibers (KF-B). The smoother and thinner fibers were effective in removing non-cellulosic components and other impurities (i.e., pectin and wax) which serve as the protective layer of KF.

The yield of KF-CNC

After acid hydrolysis process. The resulting of yield of KF-CNC was 72%, the aqueous suspension of KF-CNC was stable after hold on after 96 hours. Furthermore, the flow birefringence was carried out under a cross-polarized light setup, that specified the particle of cellulose in the KF-CNC aqueous suspension. Table 3 show the aqueous suspension, given hydrolysis condition, under normal light and under cross-polarized light.

Table 3 Hydrolysis and KF-CNC synthesis.

KF-CNC (Deep yellow, translucent solution Yield = 72%)		
normal light	**polarized light**	**CNC gel**
		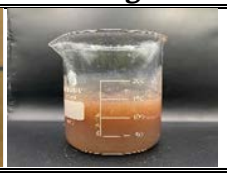

TEM Morphology KF-CNC

Figure 4a and 4b show the TEM image of KF-CNC under acid hydrolysis condition. The KF-CNC was of whisker shape as the acid remove the amorphous region of KF-B while retaining the straight crystalline regions. The length and diameter of KF-CNC show in nano scale. The reduce size of KF-CNC effective from amorphous domain was remove after acid hydrolysis.

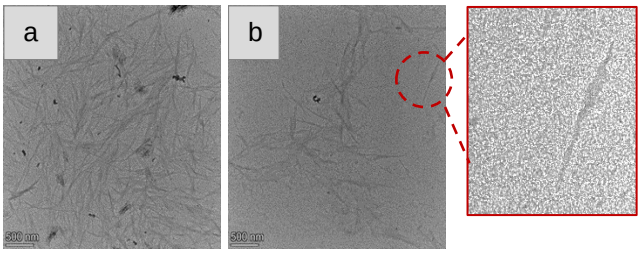

Figure 4 Morphology of KF-CNC (a,b) observed using a transmission electron microscope (TEM).

NMR chemical composition

Figure 5a-5c present the NMR curves of KF, KF-B, and KF-CNC, respectively. The peak at 17, 52, and 148 were hemicellulose and lignin. However, all peaks with lignin and hemicellulose disappeared after alkalization and bleaching, which meansthe alkalization and bleaching effectively removed hemicellulose and lignin.

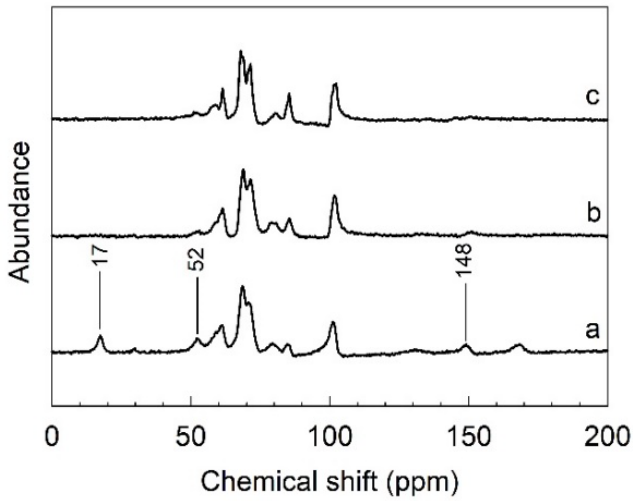

Figure 5 NMR spectrum of (a) KF, (b) KF-B, (c) KF-CNC.

FTIR chemical composition

Peaks for RF found in the FTIR microscopy results are 1209, 1270, and 1502 cm^{-1} (Figure 6). On the other hand, it was observed that the apparent peak gradually faded as more KF-CNC was added to create CRF. It may be possible that a peak point significantly disappeared as a result of KF-CNC filling into RF.

Morphology of RF and CRF

CRF was produced by using a natural rubber latex composite with varying KF-CNC (0 phr, 2.5 phr, and 5 phr). Figure 7a-7d shows the cell structures of RF and CRF. Figure 7a shows the cell structure of RF as a big hole and a close cell. Besides, after adding KF-CNC as shown in Figure 7B-7C.

DOI: 10.60101/jarst.2023.254006

JOURNAL OF APPLIED RESEARCH ON SCIENCE AND TECHNOLOGY

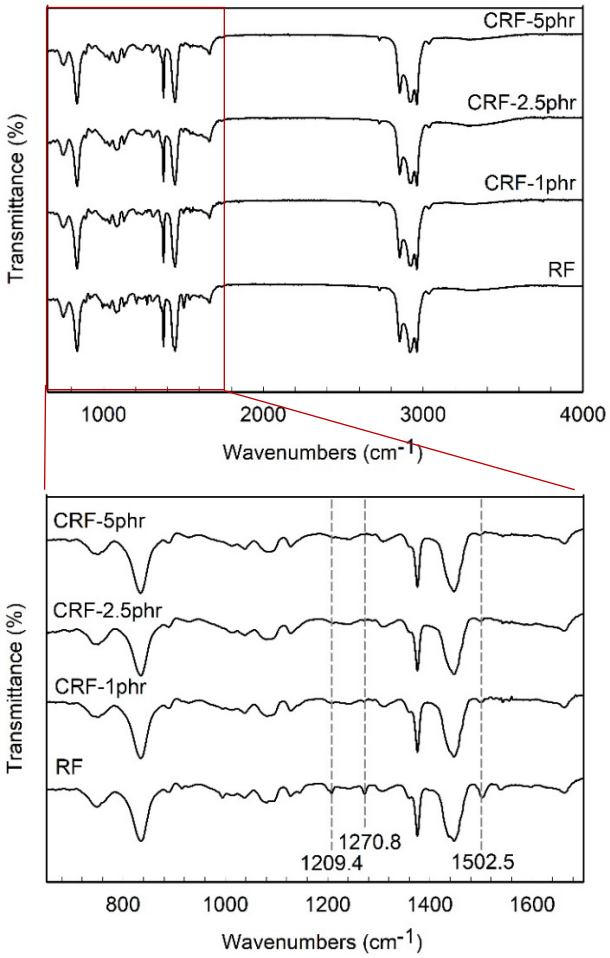

Figure 6 FTIR spectrum of RF and CRF.

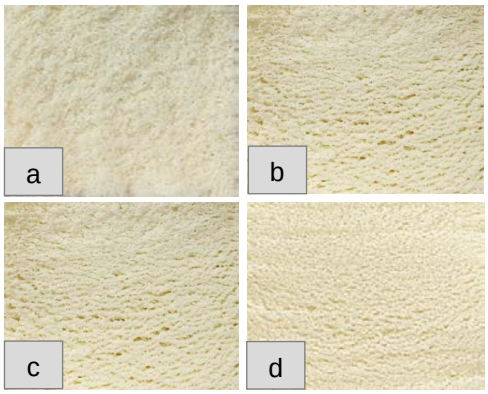

Figure 7 Cell structure of RF and CRF (a) RF, (b) CRF-1phr, (c) CRF-2.5phr, (d) CRF-5phr.

Figure 8a-8d shows the properties of RF and CRF at 0, 1, 2.5, and 5 phr respectively. Figure 8a show average hole size of RF is 400 µm, which bigger than KF-CNC (Figure 8b-8Dd) were show average hole size is 200 µm. the cell structure of RF and CRF is open cell. That has good properties for oil absorption.

Compression test result of RF and CRF

The percentage of CRF compression decreased. When the concentration of KF-CNC was increased (Figure 9). Compression % it shows that 1 phr is better than 2.5 and 5 phr because 1 phr is soft, but 2.5phr and 5phr are hard, which may result in poor oil retention performance. However, the results are not significantly different since the size of cellulose at the nanoscale appears tiny. It is possible that the smaller cellulose will not affect the bubble cells in the RF as much as the larger cellulose will.

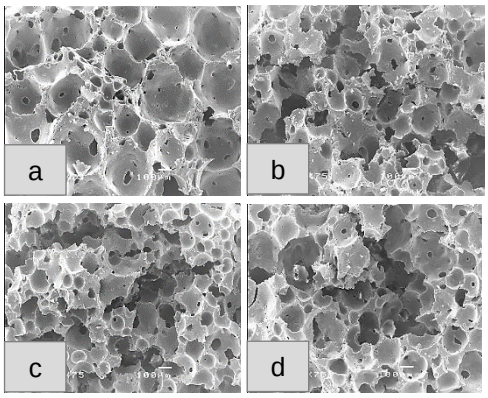

Figure 8 SEM micrographs 75x of RF and CRF composites (a) RF, (b) CRF-1phr, (c) CRF-2.5phr, (d) CRF-5phr.

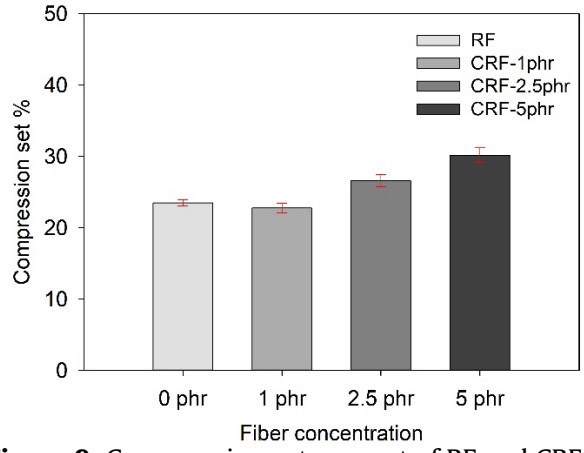

Figure 9 Compression set percent of RF and CRF.

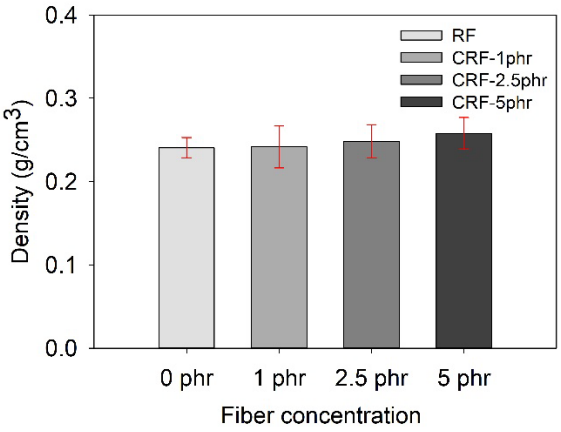

Figure 10 Density of RF and CRF.

Density test results of RF and CRF

Figure 10 shows the density comparison between RF and CRF. The density of RF (excluding

DOI: 10.60101/jarst.2023.254006

KF-CNC) is notably lower due to its larger pore sizes. On the other hand, the density of CRF exhibits a direct correlation with the volume of KF-CNC incorporated. As the quantity of KF-CNC is augmented, it contributes to the overall weight of the CRF, consequently leading to an increase in its density. This phenomenon is attributed to the introduction of KF-CNC, which possesses a denser composition compared to CRF.

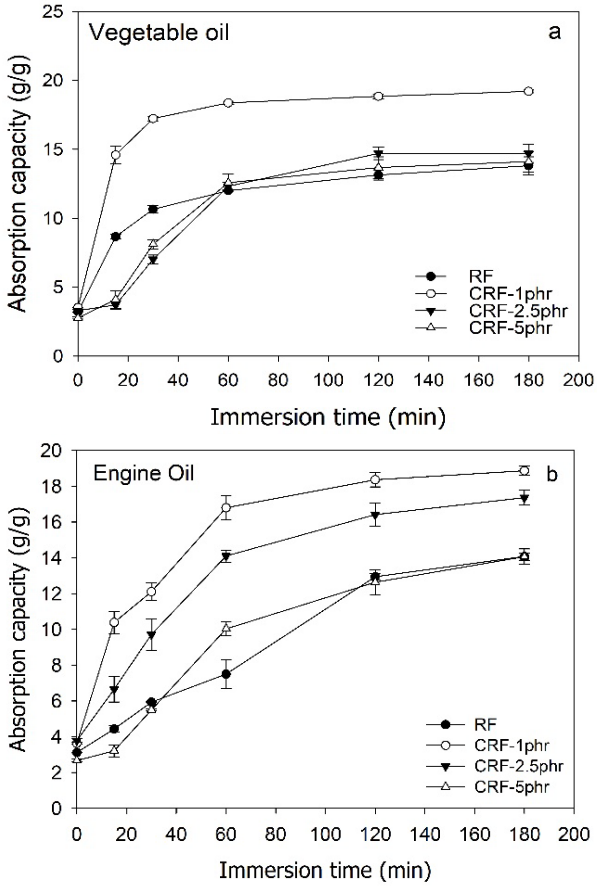

Figure 11 Absorption capacity of RF and CRF. From the graph (a) vegetable oil and (b) engine oil.

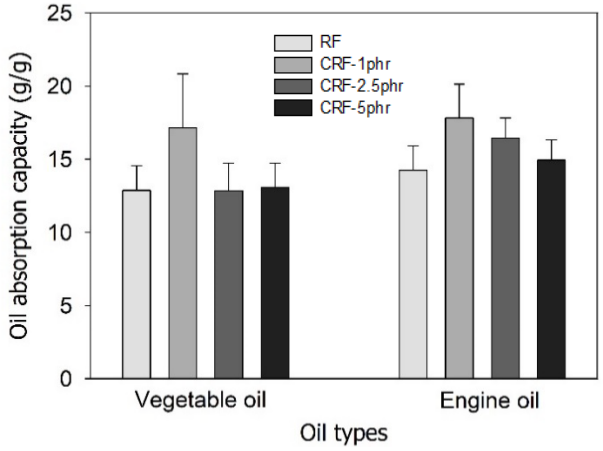

Figure 12 Oil absorption capacity of RF and CRF. From the graph shows vegetable oil and engine oil.

Oil absorption capacity of RF and CRF

Figure 11 shows the oil absorption of both oils. It can be seen that CRF-1phr (6.8-11.1 g/g) had higher oil absorption in the first 15 minutes compared to RF (1.3-5.5 g/g), CRF-2.5phr (0.4-2.9 g/g), and CRF-5 phr (0.5-1.3 g/g), but CRF absorbs more oil than RF for 60 minutes or more (Figure 12). CRF-1phr (17.1-17.8 g/g) absorbs the most of both oils. Probably because KF-CNC makes the material porous enough to absorb oil when filled. The use of particles as additives, such as nanoparticles, is generally limited to foams. Because the foams are in a solid state during the oil or solvent absorption and extraction processes, the additive materials (in varying particle sizes) and the different sizes of pores in the foam play an essential role in defining the foam's absorption capacity. It is widely acknowledged that smaller nanoparticles and pores, i.e., smaller regions, have a more highly active surface area and boundaries. The considerably smaller size of the foam particles and pores aids in the molecular interactions of the adsorbate ions and groups for improved oil and solvent absorption ability [11].

The absorption of RF and CRF (CRF-1phr) in water is shown in Figure 13. RF and CRF-1phr absorbed with time intervals of 15, 30, 60, 120, and 180 minutes. The CRF-1phr were adsorbent absorbs more oil. Furthermore, the chart shows that RF and CRF do not absorb water but instead prefer to absorb oil first.

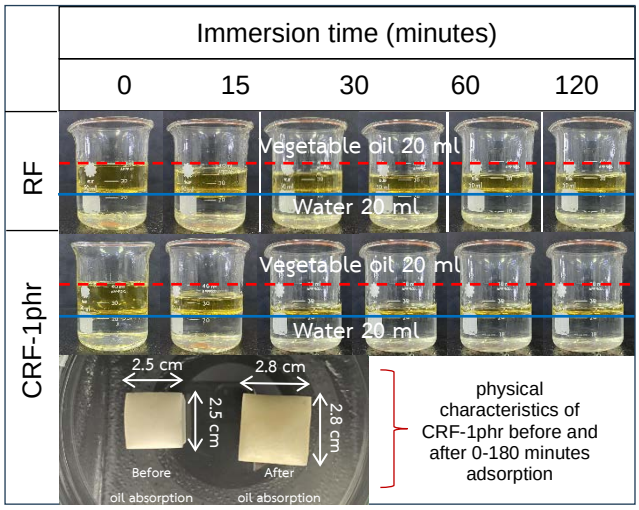

Figure 13 Absorption capacity of RF and CRF-1phr in water. The table shows the vegetable oil and physical characteristics of CRF-1 phr before and after 0-180 minutes adsorption.

Reusability of the CRF

CRF-1phr, the result of oil absorption by CRF, was selected to test the reusability of the material since it absorbs both types of oil the best (Figure 14) [12]. More than 50 times can be used with one CRF-

DOI: 10.60101/jarst.2023.254006

JOURNAL OF APPLIED RESEARCH ON SCIENCE AND TECHNOLOGY

1phr. Absorbs between 337.8 (Engine oil) and 553.4 (Vegetable oil) g/g without noticeably losing any of its quality over time. The difference in oil absorption between the two types of RF and CRF could be explained that the viscosity of Engine oil at the same temperature was lower than that of vegetable oil which was conducive to oil penetration into the porous skeleton of the RF and CRF. However, the low viscosity of the engine oil produced a negative effect on its adherence to the cellulose skeleton of the RF and CRF, resulting in a reduction in the amount of oil maintained in the RF and CRF [13].

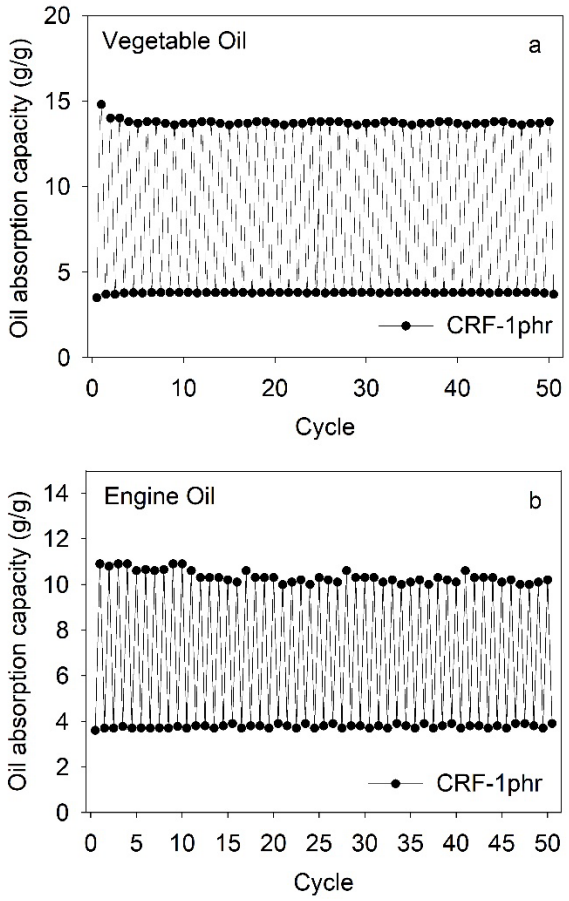

Figure 14 Reusability of CRF. From the graph (a) vegetable oil and (b) engine oil.

CONCLUSIONS

Results from KF and KF-CNC preparation

Chemical processes can be used to produce KF. Hydrogen peroxide and sodium hydroxide were used as the chemical treatments. According to the results of the morphological tests, chemical cleaning made the fibers purer than those seen with a scanning electron microscope (SEM), and the fact that KF are nanometer-sized indicates that hydrolysis can reduce the fiber size down to the nanometer level observed with a transmission electron microscope (TEM). On the NMR curve, it can be noticed that there are 17, 52, and 148 ppm of missing waves after the line improvement by chemical technique. This demonstrates that the fiber is purer in terms of fiber enhancement by chemical techniques. The end product of five centrifugations is KF-CNC water, which is produced by spinning at 9,000 rpm for 10 minutes at 25 °C. And a 72% yield of KF-CNC can be obtained by centrifuging it at 10°C for 50 minutes.

Results from RF and CRF preparation

The properties of RF and CRF at densities of 0, 1, 2.5, and 5 phr appear in the morphological results of RF and CRF from SEM micrographs 75x. It was discovered that the foam cell structure had an open-cell morphology. When KF-CNC and RF are mixed, the KF-CNC is scattered throughout the rubber foam, where the KF-CNC position is scattered freely. The spread of KF-CNC makes it harder to produce large air bubbles, resulting in smaller foam porosity [14].

RF peaks were observed in the FTIR microscopy data at 1209.4, 1270.8, and 1502.5 cm^{-1}. To produce CRF, however, CNC was added, and it was seen that the apparent peak progressively vanished. The amount of KF-CNC employed in the study was chosen at 0, 1, 2.5, and 5 phr to make CRF. It was discovered that as the amount of KF-CNC grows, the density of CRF increases. Compression % in CRF reduced. When the concentration of KF-CNC was raised. In the oil absorption test for both vegetable oil and engine oil, it was discovered that at 1 phr (CRF-1phr), it absorbs more oil (17.1-17.8 g/g) and faster in the first 15 minutes, and it can also be reused more than 50 times. The adsorbed content ranged from 337.76 to 553.33 g/g and did not absorb water but instead preferred to absorb oil first. The difference in oil absorption between the two types of RF and CRF from the decrease in compression % shows that 1 phr is soft, but 2.5 phr and 5 phr are hard, causing poor oil retention performance.

ACKNOWLEDGEMENT

The research project funded by the fundamental fund (FF) of Rajamangala University of Technology Thanyaburi under the annual research and innovation promotion fund 2022 (FRB65E0708) was created and achieved with the encouragement and assistance of many individuals and associations, to whom the researchers should be grateful on this occasion.

REFERENCES

1. Phomrak S, Nimpaiboon A, Newby B-mZ, Phisalaphong M. Natural rubber latex foam reinforced with micro- and nanofibrillated cellulose via Dunlop method. Polymers. 2020;12(9):1959.
2. Karim AFA, Ismail H, Ariff ZM. Properties and characterization of kenaf-filled natural rubber latex foam. BioResources. 2016;11(1):1080-91.
3. Kengkhetkit N, Amornsakchai T. Utilisation of

DOI: 10.60101/jarst.2023.254006

pineapple leaf waste for plastic reinforcement: 1. A novel extraction method for short pineapple leaf fiber. Ind Crop Prod. 2012;40:55-61.

4. Dong T, Xu G, Wang F. Oil spill cleanup by structured natural sorbents made from cattail fibers. Ind Crop Prod. 2015;76:25-33.
5. Lee BM, Jeun JP, Kang PH, Choi JH, Hong SK. Isolation and characterization of nanocrystalline cellulose from different precursor materials. Fiber Polym. 2017;18:272-7.
6. Arnata IW, Suprihatin S, Fahma F, Richana N, Candra Sunarti T. Cellulose production from sago frond with alkaline delignification and bleaching on various types of bleach agents. Orient J Chem. 2019;35(1):8-19.
7. Pantamanatsopa P, Ariyawiriyanan W, Ekgasit S. Production of Cellulose Nanocrystals Suspension with High Yields from Water Hyacinth. J Nat Fibers. 2023;20(1):2134266.
8. 395 AD. Standard test method for rubber property-compression set of vulcanized rubber. 1955.
9. Yuan Y, Shutov F. Foam-in-foam polyurethane composite. J Cell Plast. 2002;38(6):497-506.
10. 726-12 Standard Test Method for Sorbent Performance of Adsorbents 2012. ASTM F, editor. ASTM Philadelphia.
11. Dilamian M, Noroozi B. Rice straw agri-waste for water pollutant adsorption: Relevant mesoporous super hydrophobic cellulose aerogel. Carbohydr Polym. 2021;251:117016.
12. Ratcha A, Samart C, Yoosuk B, Sawada H, Reubroycharoen P, Kongparakul S. Polyisoprene modified poly (alkyl acrylate) foam as oil sorbent material. J Appl Polym Sci. 2015;132(42).
13. Udayakumar KV, Gore PM, Kandasubramanian B. Foamed materials for oil-water separation. Chemical Engineering Journal Advances. 2021;5:100076.
14. Yousefian H, Rodrigue D. Morphological, physical and mechanical properties of nanocrystalline cellulose filled Nylon 6 foams. J Cell Plast. 2016;53(3):253-71.

DOI: 10.60101/jarst.2023.254006